Tribol Lett (2008) 31:119–128
DOI 10.1007/s11249-008-9344-z

ORIGINAL PAPER

The Influence of Anchoring-Group Structure on the Lubricating Properties of Brush-Forming Graft Copolymers in an Aqueous Medium

Whitney Hartung · Tanja Drobek · Seunghwan Lee · Stefan Zürcher · Nicholas D. Spencer

Received: 14 May 2008 / Accepted: 10 July 2008 / Published online: 26 July 2008

Abstract We have compared the lubricating properties of two different PEG-grafted, polycationic, brush-forming copolymers to gain a deeper understanding of the role of the polyionic backbone in the lubricating behavior of such materials, when used as additives in aqueous lubricant systems. Previously, poly(L-lysine)-*graft*-poly(ethylene glycol) (PLL-*g*-PEG) has been shown to adsorb onto oxide surfaces from aqueous solution and substantially lower frictional forces. Poly(allylamine)-*graft*-poly(ethylene glycol) (PAAm-*g*-PEG), which also has a polycationic backbone, has been synthesized in several different architectures, and its performance investigated via adsorption tests, rolling- and sliding-contact tribometry, and the surface forces apparatus. These tests show a clear reduction of friction forces with PAAm-*g*-PEG compared to water alone. However, when compared with PLL-*g*-PEG, while PAAm-*g*-PEG copolymers did not adsorb to the same extent or exhibit as high a lubricity in sliding geometry, they showed a similar lubricating effect under rolling conditions. The difference in the chemical structure of the backbones, especially the flexibility of the anchoring groups, appears to significantly influence both the extent and kinetics of polymer adsorption, which in turn influences lubrication behavior.

Keywords
Poly(allylamine)-*g*-poly(ethylene glycol) (PAAm-*g*-PEG) · Poly(L-lysine)-*g*-poly(ethylene glycol) (PLL-*g*-PEG) · Aqueous lubrication · Polymer architecture · Polymer brush · Boundary lubrication · Anchoring groups

W. Hartung · T. Drobek · S. Lee · S. Zürcher · N. D. Spencer (✉)
Department of Materials, Laboratory for Surface Science and Technology, ETH Zurich, Wolfgang-Pauli-Strasse 10, 8093 Zurich, Switzerland
e-mail: spencer@mat.ethz.ch

1 Introduction

Poly(ethylene glycol) (PEG) brushes have been shown in many recent publications to be highly lubricious when saturated with water [1–15]. In particular, the modification of oxide surfaces with the cationic brush-like copolymer poly(L-lysine)-*graft*-poly(ethylene glycol) (PLL-*g*-PEG) has been shown to significantly lower frictional forces between these surfaces in an aqueous environment [4, 5, 7–15]. PLL-*g*-PEG incorporates a polycationic backbone of poly(L-lysine) (PLL), which adsorbs from aqueous solution onto negatively charged surfaces, such as those of many oxides [4, 5, 7–38], establishing electrostatic interactions at multiple sites along the backbone. Compared to other grafting methods, e.g., silane-PEG grafted onto oxide surfaces [24], higher PEG chain surface densities can be readily achieved due to the radial distribution of PEG side chains along the PLL in aqueous solution, which, upon adsorption of the backbone, extend away from the surface. By controlling the PEG spacing along the backbone, the resulting PEG surface density can be tailored prior to adsorption [5, 17, 24]. Surface attachment via a long polycationic backbone, rather than covalently linking the PEG chains to the surface, leads to an advantageous self-healing effect [10], by which the electrostatically adsorbed protective brush layer, if removed under tribological contact, readsorbs.

Past work has also shown the importance of the grafting ratio, defined as the number of lysine units per grafted PEG chain; if too high, the PEG density on the surface is too low to produce the desired tribological effects; if too low, too few charges remain on the backbone for the brush to adsorb on the surface [5, 17, 24]. Tribological studies have revealed that, for tribological applications, PEG side-chain lengths of 5 kDa provide optimal tribological properties, and optimal adsorption properties for 5 kDa side chains

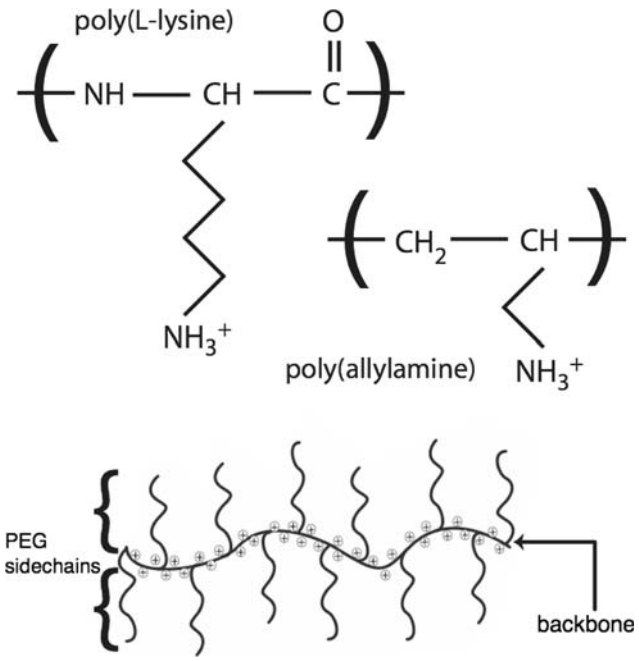

Fig. 1 Structure of poly(L-lysine) and poly(allylamine), and schematic structure of a brush-like graft copolymer with a polycationic backbone and a grafting ratio of 4

require a PLL backbone length of 20 kDa and a grafting ratio around 3–5 [5].

In this study, the effects of the chemical structure of the anchoring groups are explored via tribological testing and surface analysis. We introduce another brush-like PEG-based copolymer, poly(allylamine)-*graft*-poly(ethylene glycol) (PAAm-*g*-PEG). This copolymer is similar to PLL-*g*-PEG, except the PLL backbone is replaced with poly(allylamine) (PAAm), as shown in Fig. 1. Both PLL and PAAm ionize via protonation of amine groups; however, there are important differences between PAAm and PLL. First, the PAAm repeat unit is significantly shorter: 2.8, compared to 3.6 Å for PLL.[1] Second, the structure of the anchoring groups differs significantly; the protonated primary amine group of PLL lies at the end of a C_4 hydrocarbon chain ($-CH_2CH_2CH_2CH_2NH_3^+$), whereas that of allylamine is connected via a single methylene unit ($-CH_2NH_3^+$), as shown in Fig. 1. The presence of the relatively long C_4 hydrocarbon chain, in the case of PLL, provides additional degrees of freedom in the position of the amine group [39].

Investigations of PAAm-*g*-PEG copolymers with backbone lengths of 14 kDa, grafting ratios between 2.5 and 6.5, and PEG side chain lengths of 5 kDa, as well as a previously determined optimal architecture of PLL-*g*-PEG [6], are reported in this work. One additional polymer with a longer 70 kDa backbone and a grafting ratio of 3.5 (PAAm(70)-*g*[3.5]-PEG(5), meaning a PAAm backbone of 70 kDa, PEG side chains of 5 kDa, and a grafting ratio of 3.5) has also been included, to investigate possible effects of longer backbone lengths, which may not lie flat on the surface. Adsorption experiments were performed by means of optical waveguide lightmode spectroscopy (OWLS). Rolling and sliding tribometry experiments were carried out to examine the lubricating behavior of the various copolymers under different tribological conditions. Finally, a surface forces apparatus (SFA) was used to determine the equilibrium brush thickness of several of the adsorbed copolymers.

[1] as calculated with ChemDraw version 10.0 (CambridgeSoft, Cambridge, Massachusetts, USA).

2 Experimental Details

2.1 Synthesis of Poly(allylamine)-*graft*-poly(ethylene glycol) and poly(L-lysine)-*graft*-poly(ethylene glycol)

PAAm-*g*-PEG and PLL-*g*-PEG were synthesized via a similar route; complete details of the synthesis of PLL-*g*-PEG can be found in previous publications [16, 40]. Briefly, poly(allylamine) hydrochloride or poly(L-lysine) hydrobromide (both from Fluka, Switzerland) of the desired backbone molecular weight (PAAm: 14 or 70 kDa, PLL: 20 kDa, including the Cl^- or Br^- counterion) were dissolved at a concentration of 100 mM in a 50 mM sodium borate buffer solution adjusted to pH 8.5. The solution was filtered through a 0.22 μm filter. To graft PEG onto PLL or PAAm, the N-hydroxysuccinimidyl ester of methoxy-poly(ethylene glycol) propionic acid (mPEGSPA, Nektar, Huntsville, AL, USA) was added to the PLL-HBr or PAAm-HCl solution. The reaction was allowed to proceed for 6 hours at room temperature, after which the reaction mixture was dialyzed (Spectra-Por, molecular weight cutoff size 6–8 kDa, Spectrum, Houston, TX, USA) for 48 h against deionized water. The product was freeze-dried and stored in powder form at –20 °C. Detailed information about the molecular weight and structure can be found in Table 1.

For all macroscopic tribometry experiments described in this article, PLL-*g*-PEG and PAAm-*g*-PEG were dissolved at a concentration of 0.25 mg/mL in an aqueous buffer solution consisting of 10 mM 4-(2-hydroxyethyl)piperazine–1-ethanesulfonic acid (HEPES, Fluka, Switzerland) adjusted to pH 7.4 using the appropriate amount of a 6.0 M NaOH solution (less than 1 mL/L, corresponding to a change of <1% in the ionic strength).

2.2 Adsorption Measurements with Optical Waveguide Lightmode Spectroscopy (OWLS)

OWLS is a method that, by means of the evanescent field of a waveguide-incoupled He–Ne laser, can probe the mass

Table 1 The structure of the (co)polymers employed in this work

(Co)polymer	(Backbone) molecular weight (kDa)		Total molecular weight (kDa)	Number of repeat units		Number of backbone free amine groups	Number of grafted PEG chains
	With counterion	Without counterion		Backbone	Side chains		
PAAm(14)	14	8.6	–	151	–	–	–
PAAm(70)	70	43	–	757	–	–	–
PEG(5)	5	5	–	81	–	–	–
PLL(20)	20	13	–	89	–	–	–
PAAm(14)-g[2.5]-PEG(5)	14	8.6	311	151	81	91	61
PAAm(14)-g[3.5]-PEG(5)	14	8.6	225	151	81	108	43
PAAm(14)-g[4.5]-PEG(5)	14	8.6	177	151	81	118	34
PAAm(14)-g[5.5]-PEG(5)	14	8.6	146	151	81	124	28
PAAm(14)-g[6.5]-PEG(5)	14	8.6	125	151	81	128	23
PAAm(70)-g[3.5]-PEG(5)	70	43	1,124	757	81	540	216
PLL(20)-g[2.9]-PEG(5)	20	13	166	89	81	58	31

of adsorbed macromolecules on a waveguide to an accuracy of 2 ng/cm^2 [41]. The OWLS 110 (MicroVacuum, Budapest, Hungary) was used to perform adsorption measurements on uncoated $Si_{0.25}Ti_{0.75}O_2$ waveguides (MicroVacuum, Budapest, Hungary).

The waveguides were ultrasonicated in 0.1 M HCl for 10 min, rinsed thoroughly with ultrapure water (Millipore, Billerica, Massachusetts, USA), ultrasonicated in isopropanol for 10 min, dried in an N_2 stream, and UV/O_3 cleaned for 30 minutes. Following assembly of the flow cell, HEPES buffer was injected, and the baseline was allowed to stabilize for at least 30 min. The copolymer solution (described in Sect. 2.1) was then injected and allowed to adsorb for 30 min. HEPES was then injected once every 10 min for 30 min to remove all loosely bound copolymer from the surface. This value was taken as the adsorbed mass of the copolymer. Values for dn/dc, where n is the refractive index and c is the concentration, calculated for each copolymer using measured values for PLL (0.18 cm^3/g) and PEG (0.13 cm^3/g), and a measured value of dn/dc for PAAm (0.23 cm^3/g) are shown in Table 1.

2.3 Mini-Traction Machine (MTM)

An MTM (PCS Instruments London, United Kingdom) was employed to characterize the lubricating properties of the copolymer solutions under rolling-contact conditions. The MTM measures the frictional forces between a ball and a disk, each of which can be rotated independently at different speeds. All of the measurements performed in this work were taken at a slide-roll ratio (SRR), defined as the sliding speed divided by the entrainment speed as in Eq. 1 (in which v_{ball} is the velocity of the ball and v_{disk} is the velocity of the disk), of 10%. Specimens included glass disks (46-mm diameter, 6-mm thick) machined by Qualicut AG

$$\mathrm{SRR} = 2 \cdot \frac{v_{ball} - v_{disk}}{v_{ball} + v_{disk}} \cdot 100\% \quad (1)$$

(Mönchaltorf, Switzerland) and AISI 52100 steel balls (19 mm diameter, PCS Instruments). The balls and disks were ultrasonically cleaned in ethanol for 10 min, and the glass disks were further cleaned in air plasma (Harrick Scientific, Ithaca, NY) for two minutes. The disk was then submerged into a buffered copolymer solution (as described in Section 2.1) for 30 min to allow the copolymer to adsorb onto the surface. Following adsorption, measurements took place at 27 °C with the disk still submerged in the buffered copolymer solution, beginning each time at the highest speed of 2,500 mm/s and gradually decreasing to 10 mm/s, yielding coefficient of friction values (μ, defined as friction/load) at various speeds.

2.4 Pin-On-Disk Tribometry

A pin-on-disk tribometer (CSM Instruments, Peseux, Switzerland), consisting of a rotating disk and stationary pin, was employed to characterize the lubricating properties of the copolymer solutions under sliding-contact conditions. Glass slides (SuperFrost extra-white electroverre glass, Menzel-Gläser, Braunschweig, Germany), cut approximately to 2.5 cm^2, were used as rotating disks, and steel balls (6 mm in diameter, DIN 5401-20 G20, Hydrel, Romanshorn, Switzerland) served as the stationary pin. Disks and pins were ultrasonically cleaned in ethanol prior to testing, and disks were subsequently cleaned in air plasma for two minutes before being placed in HEPES

buffer solution until testing. Immediately before testing, the copolymer was allowed to adsorb from the buffered copolymer solution onto the disks for 30 min, to ensure that the maximum amount of copolymer had adsorbed on the surface.

Two series of experiments were conducted, one with varying normal load and one with varying speed. The varied-load series included measurements under 5, 2, 1, and 0.5 N normal loads (corresponding to contact pressures in the range of 220–480 MPa), each on different tracks, for 50 rotations at 5 mm/s, and each set of four measurements was repeated on three separate disks. The pin was rotated slightly between each individual measurement to provide a fresh contact point each time. The varied-speed measurements consisted of 20 rotations under 2 N (approximate contact pressure 350 MPa) at 19, 15, 10, 5, 2, and 1 mm/s. Each set of six speeds was performed on the same radius, and each set of measurements was repeated on two new disks. The pin was rotated only when the disk was changed.

2.5 Surface Forces Apparatus (SFA)

For the SFA experiments, an enhanced and automated version of the MARK 3 (Surforce, Santa Barbara, CA), described fully in other publications [18], was used. The mica surfaces were prepared following a procedure described elsewhere [30]. Prior to the adsorption of the copolymers, the thickness of the mica surfaces was determined interferometrically in the SFA.

Two different architectures of the PAAm-*g*-PEG copolymer were used for the experiment. For the ex situ adsorption process, both the surfaces were immersed in a solution of the copolymer each time. After removal they were thoroughly rinsed with a jet of ultrapure water and mounted in the SFA with a drop of solvent between the surfaces. In case of PAAm(14)-*g*[6.5]-PEG(5) a solution of 0.5 mg/mL in HEPES buffer and an immersion time of 40 min were used, and the surfaces were mounted with a drop of buffer solution between them. For the PAAm(70)-*g*[3.5]-PEG(5) a solution of 0.1 mg/mL in ultrapure water (puris. p.a., Fluka, Milwaukee, WI) and an immersion time of 75 min were used, the surfaces being subsequently mounted with a drop of ultrapure water between them.

The data were compared with results for PLL(20)-*g*[2.9]-PEG(5) and PLL(20)-*g*[3.5]-PEG(5). These were taken from a series of experiments described in [12, 30].

Compression isotherms were carried out at 25.0 °C with a measuring spring of 500 N/m and motor speeds of 5 and 10 nm/s. These relatively high speeds were chosen to reduce systematic errors due to drift induced by the unavoidable evaporation of the solvent.

3 Results

3.1 OWLS

Adsorbed mass per unit area versus grafting ratio of both PLL-*g*[2.9]-PEG(5), PAAm(70)-*g*[3.5]-PEG(5), and PAAm(14)-*g*[*x*]-PEG(5), as systematically studied with OWLS, is shown in Fig. 2. PAAm(70)-*g*[3.5]-PEG(5) showed the highest level of adsorption among the PAAm-based polymers (154 ± 2 ng/cm^2). Adsorbed copolymer mass ranged from 84 ± 17 ng/cm^2 for a grafting ratio of 4.5 to 126 ± 14 ng/cm^2 for a grafting ratio of 6.5. Although a general trend of increased amount of adsorption can be seen with increasing grafting ratios, no significant difference in adsorbed amount can be seen at grafting ratios from 2.5 to 4.5. Also interesting to note is that the adsorbed mass for grafting ratios 5.5 and 6.5 were still lower than the average adsorption of PLL-*g*-PEG with the lower grafting ratio of 2.9 (156 ± 39 ng/cm^2).

Adsorbed mass, as well as the conformational factors calculated from the adsorbed mass and copolymer structure, is provided in Table 2. To better assess the efficacy of surface grafting of PEG chains for different polymer architectures, the areal density of PEG chains n_{PEG} (Eq. 2) was calculated, as described in a previous publication [24]. The quantity m_{adsorbed} is the adsorbed mass per unit area measured by OWLS, M_{backbone} is the molecular weight of one backbone repeat unit (not including the counterion), g represents the grafting ratio, and M_{PEG} is the molecular weight of one PEG side chain, M_{EG} is the molecular weight of one EG repeat unit, and N_{A} is Avogadro's number.

$$n_{\mathrm{PEG}} = \frac{m_{\mathrm{adsorbed}} \cdot N_{\mathrm{A}}}{M_{\mathrm{backbone}} \cdot g + M_{\mathrm{PEG}}} \tag{2}$$

Similarly, the areal density of copolymer molecules (n_{brush}) on the surface was calculated via a related equation

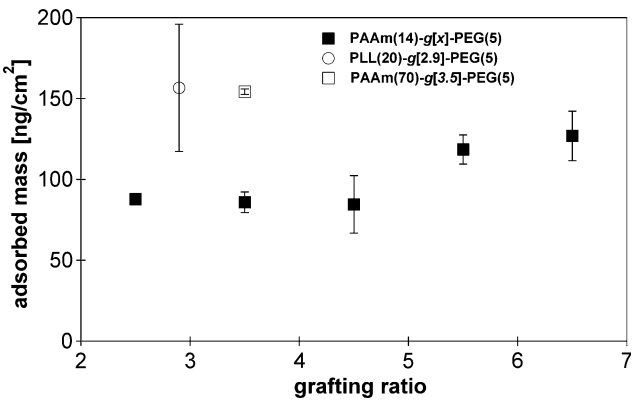

Fig. 2 Adsorbed mass of PAAm(14)-*g*-PEG of various grafting ratios, as well as PAAm(70)-*g*[3.5]-PEG(5) and PLL(20)-*g*[2.9]-PEG(5), measured with OWLS on uncoated $SiO_{0.25}/Ti_{0.75}O_2$ waveguide surfaces in 10 mM HEPES buffer. In every case the mass of adsorbed PAAm(14)-*g*-PEG(5) is somewhat lower than that of PLL(20)-*g*[2.9]-PEG(5)

Table 2 Summary of adsorption data of PAAm-*g*-PEG as measured by OWLS

Copolymer	d*n*/d*c*[a]	Adsorbed mass (ng/cm^2)	n_{PEG}[b] (1/nm^2)	n_{Brush}[c] ($1\cdot10^{-5}$/nm^2)	Mean distance between PEG chains along backbone[d] (Å)	Relative packing factor[e] ($L/2R_g$)
PAAm(14)-*g*[2.5]-PEG(5)	0.137	87 ± 3	0.10 ± 0.004	1.7 ± 0.1	7.0	0.73 ± 0.03
PAAm(14)-*g*[3.5]-PEG(5)	0.139	85 ± 6	0.099 ± 0.007	2.4 ± 0.2	9.8	0.74 ± 0.05
PAAm(14)-*g*[4.5]-PEG(5)	0.142	84 ± 17	0.10 ± 0.02	3.0 ± 0.6	12.6	0.75 ± 0.15
PAAm(14)-*g*[5.5]-PEG(5)	0.144	118 ± 8	0.13 ± 0.02	5.2 ± 0.4	15.4	0.64 ± 0.05
PAAm(14)-*g*[6.5]-PEG(5)	0.147	127 ± 14	0.14 ± 0.02	6.6 ± 0.7	18.2	0.61 ± 0.07
PAAm(70)-*g*[3.5]-PEG(5)	0.139	154 ± 2	0.178 ± 0.002	0.83 ± 0.01	9.8	0.55 ± 0.01
PLL(20)-*g*[2.9]-PEG(5)	0.139	157 ± 39	0.18 ± 0.05	5.7 ± 1	10.4	0.55 ± 0.14

[a] d*n*/d*c* represents the change of the index of refraction with changing concentration

[b] n_{PEG} is the number of PEG chains on the surface per unit area, calculated from the adsorbed mass of the polymer

[c] n_{Brush} is the number of copolymer molecules adsorbed per unit area, calculated from the adsorbed polymer mass

[d] Estimated as grafting ratio × monomer length

[e] $L/2R_g$ is the relative packing factor of the polymers adsorbed on the surface, taking into account L (average spacing between PEG side chains on the surface) and R_g (radius of gyration of PEG chains). Lower values of $L/2R_g$ suggest a higher degree of PEG side-chain overlap, leading to a more extended brush-like arrangement of PEG side chains [16, 24]

(Eq. 3), in which M_{brush} is the calculated molecular weight of the copolymer.

$$n_{brush} = \frac{m_{adsorbed} \cdot N_A}{M_{brush}} \quad (3)$$

The estimated distance between PEG side chains along the backbone was calculated as the grafting ratio multiplied by the backbone repeat length (2.8 and 3.6 Å for PAAm and PLL, respectively). Finally, the relative packing factor $L/2R_g$ [17, 24] is also included, which indicates the degree of overlap of the PEG chains on the surface. Lower values of $L/2R_g$ suggest a higher degree of PEG side-chain overlap, leading to, due to steric effects, a brush that extends further from the surface and better protection from asperity contact [5]. The calculation assumes extended backbones parallel to the surface and PEG chains, for which the radius of gyration of the isolated PEG chains, R_g, was calculated with an empirical formula based on light-scattering measurements [42]:

$$R_g = 0.181N^{0.58}\,(\text{nm}) \quad (3)$$

where N is the number of EG repeat units. R_g for 5 kDa PEG is thus 2.3 nm. The average spacing between the PEG side chains on the surface, L, is calculated as follows [17, 24]:

$$L = \left(\frac{2}{\sqrt{3}\cdot n_{PEG}}\right)^{0.5} \quad (4)$$

As seen in Table 2, there is a general increase in the n_{PEG} with increasing grafting ratio and a decrease in the relative packing factor $L/2R_g$. Despite the lower grafting ratio of PLL-*g*-PEG it has a lower relative packing factor.

3.2 MTM

Plots of μ versus speed obtained at a slide-roll ratio of 10% are shown in Fig. 3. For clarity, only the results for PAAm(14)-*g*[6.5]-PEG(5) are shown, although all PAAm-*g*-PEG architectures performed similarly to each other, and lower values of μ were observed than for HEPES buffer. Virtually no difference in the μ values was found for PAAm(14)-*g*[6.5]-PEG(5) and PLL(20)-*g*[2.9]-PEG(5).

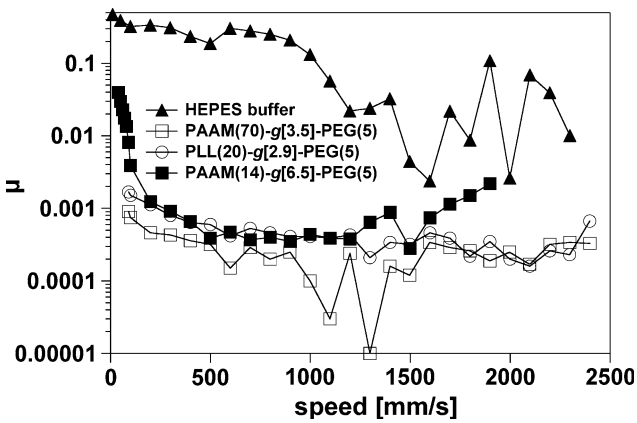

Fig. 3 Coefficient of friction versus speed plots obtained from rolling contacts lubricated by solutions of PAAm-*g*-PEG, PLL(20)-*g*[2.9]-PEG(5), and HEPES buffer. For clarity, only PAAm(14)-*g*[6.5]-PEG(5) and PAAm(70)-*g*[3.5]-PEG(5), which was tested with the SFA, are shown (see Fig. 5 for other polymer architectures). Standard deviation between measurements was in the range of ±0.005. Although there is little significant difference in the lubricity of the copolymers, they all exhibit significantly lower friction than the buffer alone

3.3 Pin-On-Disk Tribometry

μ versus speed plots and friction force versus applied load plots are shown in Fig. 4. For clarity, only the data for PAAm(14)-*g*[6.5]-PEG(5), PAAm(70)-*g*[3.5]-PEG(5), PLL(20)-*g*[2.9]-PEG(5), and HEPES are shown. As with the rolling contacts, all architectures of PAAm-*g*-PEG performed better than HEPES buffer alone and were not significantly different from each other. The μ values of PAAm-*g*-PEG (between 0.2 and 0.3) lie clearly below that of HEPES buffer (0.4–0.6), yet slightly above that of PLL-*g*-PEG (0.2 to 0.1). PAAm(70)-*g*[3.5]-PEG(5) has a slightly higher μ than that of PAAm(14)-*g*[6.5]-PEG(5), especially at speeds of 10 mm/s or faster. Figure 5 shows a comparison of the μ values in sliding and rolling contact of the various PAAm-*g*-PEG copolymers as well as PLL-*g*-PEG. All PAAm-*g*-PEG architectures show, with 2 N applied load and 5 mm/s sliding speed, sliding μ values between 0.2 and 0.3, and no significant difference can be seen between the different architectures measured. Similarly, all polymers measured at a rolling speed of 5 mm/s show only insignificant differences. Nevertheless, as seen in Fig. 4, all PAAm-*g*-PEG grafting ratios display higher sliding μ values than PLL(20)-*g*[2.9]-PEG(5).

3.4 SFA

Compression isotherm measurements carried out with the SFA revealed a predominantly repulsive interaction for all copolymer films (see Fig. 6). In the experiments carried out with a liquid drop [both data sets of PAAm-*g*-PEG, and the data set of PLL(20)-*g*[2.9]-PEG(5)], it was not possible to determine hysteretic behavior, although the scatter in the data at forces below 0.2 mN/m, caused by changes of the drift rate, may have masked weak attractive forces.

To compare the equilibrium film thickness of the different copolymers, the surface separation was determined at an arbitrary, but small, reference load of 0.6 mN/m, chosen to be just above the ambient noise level. In the case of PLL-*g*-PEG these values were shown to be in good agreement with the brush length, determined by fitting the data with a model based on the Alexander-de Gennes scaling approach [30, 43, 44]. For PAAm(14)-*g*[6.5]-PEG(5) this reveals a film thickness of 9.5 nm, whereas for

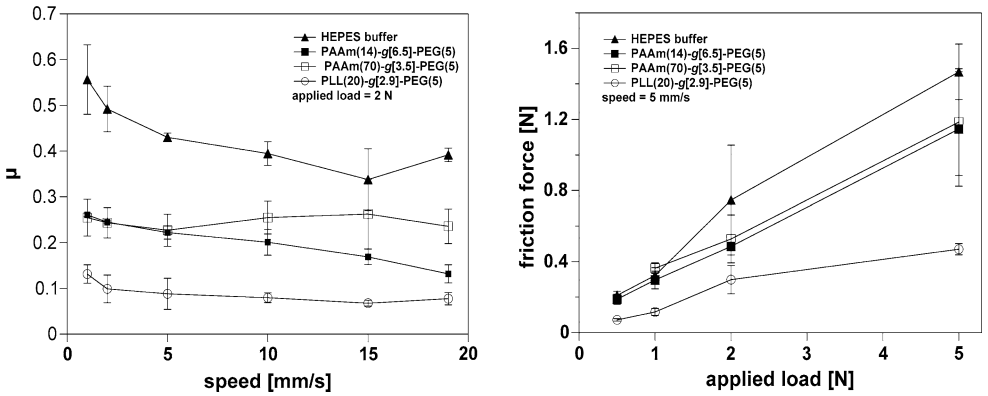

Fig. 4 Coefficient of friction versus speed plots (applied load, fixed at 2 N, speeds ranging from 1–19 mm/s) (left) and friction force versus applied load (speed, fixed at 5 mm/s, applied loads ranging from 0.5–5 N) (right) for pin-on-disk sliding tribometery, lubricated by the copolymer solutions and HEPES buffer solutions. For clarity, only PAAm(14)-*g*[6.5]-PEG(5) is shown. The μ values for all PAAm-*g*-PEG architectures studied lie between those of PLL(20)-*g*[2.9]-PEG(5) and HEPES buffer

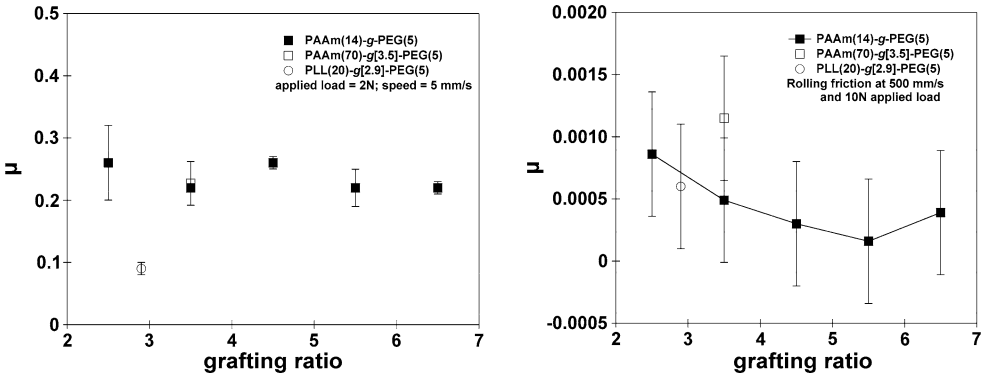

Fig. 5 Comparison of the μ values of all tested PAAm-*g*-PEG architectures, compared with PLL(20)-*g*[2.9]-PEG(5), in sliding contact (left) and rolling contact (right). There appears to be little significant difference between the various architectures of PAAm-*g*-PEG, although PLL-g-PEG exhibits significantly lower friction than PAAm-*g*-PEG under sliding-contact conditions

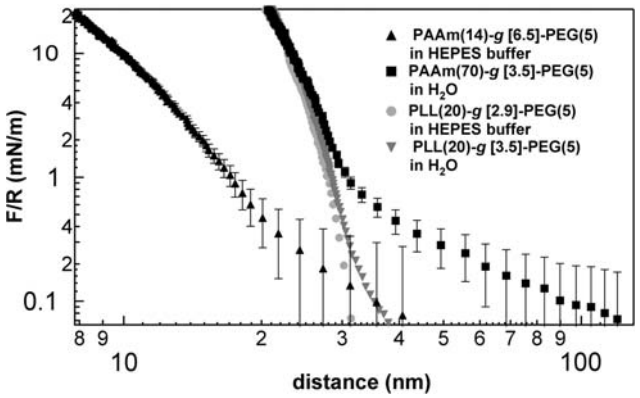

Fig. 6 Compression isotherms measured in a brush–brush conformation in the SFA for different PAAm-*g*-PEG and PLL-*g*-PEG architectures. The loading force F is normalized with the radius of curvature R of the surfaces

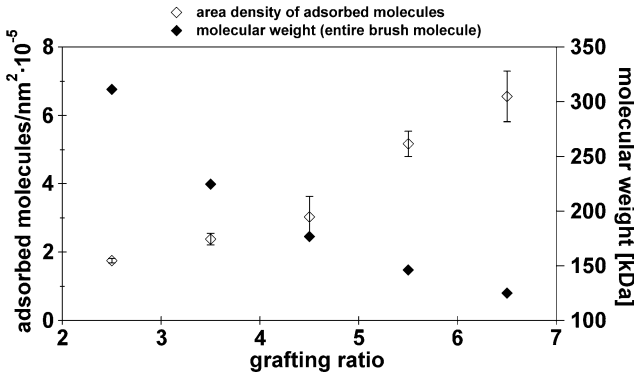

Fig 7 Number of molecules adsorbing per square nanometer and molecular weight of PAAm(14)-*g*-PEG(5)

PAAm(70)-*g*[3.5]-PEG(5) the thickness is 18 nm, and therefore comparable to the values achieved for PLL(20)-*g*[2.9]-PEG(5) (14.4 nm) and PLL(20)-*g*[3.5]-PEG(5) (16.3 nm). The error in this value is about 0.5 nm, mainly caused by scatter due to drift. For the numbers given above, an overlap of the two opposing brushes was not taken into account.

4 Discussion

Past studies have shown that the adsorption and lubrication behavior of PLL-*g*-PEG is influenced by the grafting ratio of the copolymer. The lower the grafting ratio, the more densely the PEG side chains are grafted along the backbone, yielding increased PEG surface density after adsorption to provide a steric barrier during tribocontact. However, since PEG side chains are grafted onto the amine groups of the lysines, which would otherwise provide a charge for surface bonding, too low grafting ratio leaves too few charges on the backbone for effective attachment—the energy required to push the side chains into the semi-cylindrical conformation required for adsorption cannot be overcome by the electrostatic attraction to the surface. The ideal grafting ratio for a maximum PEG coverage is therefore a balance between PEG density and charge density.

As has also been observed in the case of PLL-*g*-PEG(5) [24], the adsorbed mass of PAAm(14)-*g*-PEG(5) shows only a slight dependence on grafting ratio; as the PEG side chains become less crowded along the backbone with increasing g, an increasing number of entire molecules is able to adsorb in a given area, as illustrated in Fig. 7. Since the molecular weight of individual molecules decreases rather than increases with increasing grafting ratio, the combined effects lead to virtually constant adsorbed mass of copolymers with varying grafting ratio, especially within the range of grafting ratios 2.5–4.5. A slight increase at grafting ratios higher than 4.5 is observed, however. Similarly, in rolling and sliding friction (Fig. 5), the behavior of polymers with different grafting ratios cannot be distinguished. These results imply that the grafting-ratio range of these copolymers is appropriate for aqueous lubrication, and that the grafting ratios are below the threshold, above which the n_{PEG} begins to decrease, as was seen with PLL-*g*-PEG [24]. Nonetheless, all grafting ratios of PAAm(14)-*g*-PEG(5) adsorb to a lesser extent than does PLL(20)-*g*[2.9]-PEG(5), with only PAAm(70)-*g*[3.5]-PEG(5) adsorbing to a comparable degree.

This result is confirmed by the SFA experiments, which reveal a significantly lower equilibrium film thickness for PAAm(14)-*g*[6.5]-PEG(5) compared to PLL(20)-*g*[2.9]-PEG(5). The lower density of grafting points implies that with PAAm(14)-*g*[6.5]-PEG(5), the PEG chains are less crowded and thus less extended (more mushroom-like) [45] than in the case of the PLL(20)-*g*[2.9]-PEG(5) films. This is further reflected in Table 2, where the low value of $L/2R_g$ for PLL(20)-*g*[2.9]-PEG(5) indicates the highest degree of overlap of PEG brushes, the highest density of surface coverage, and a high extension of the PEG brushes from the surface into the aqueous solution. Due to the lower repulsive forces, the PAAm-*g*-PEG films are less effective in preventing direct solid–solid contact and maintaining a fluid film between the surfaces.

PAAm(70)-*g*[3.5]-PEG(5), with a backbone significantly longer than the PAAm(14)-*g*-PEG copolymers, showed an adsorbed mass close to that of PLL(20)-*g*[2.9]-PEG(5), but significantly higher than that of PAAm(14)-*g*-PEG(5). However, the lubrication properties are not significantly different from those of shorter PAAm(14)-*g*-PEG(4) polymers. Similarly, past studies have observed that films formed from PLL-*g*-PEG copolymers with very long (300+ kDa) PLL backbones are less effective as lubricant additives than those with shorter backbones of

20 kDa [5]. This has been assumed to be a consequence of the persistence length, since the 300 kDa backbones are more prone to loop away from the surface rather than adsorb flat, which is more likely for the 20 kD backbones [24, 29]. From ToF-SIMS analysis and neutron scattering studies of PLL(300)-*g*-PEG, it is known that such molecules tend to adsorb only partially, looping away from the surface rather than lying flat [24, 28, 38]. It is very likely that PAAm(70)-*g*[3.5]-PEG(5) molecules also adsorb with loops or ends curling away from the surface, allowing the molecules to pack more closely and increasing the total adsorbed mass. The high value of $L/2R$ for PAAm(70)-*g*[3.5]-PEG(5), normally thought to indicate more-extended side chains offering increased protection from asperity–asperity contact [5], may be misleading in the case of copolymers with longer backbone lengths, in that it does not take into account the possibility of partially adsorbed molecules. Also, despite the greater adsorbed mass of the PAAm(70)-backbone copolymer, as seen in Fig. 4, its tribological performance is poorer than that of PLL-*g*-PEG under these conditions. The higher equilibrium film thickness of PAAm(70)-*g*-PEG compared to PAAm(14)-*g*-PEG measured in SFA experiments (18 nm and 9.5 nm, respectively) additionally supports the hypothesis that the high degree of adsorption of the PAAm(70)-*g*[3.5]-PEG(5) is caused by the ends of the copolymer curling away from the surface.

The effects of the lower adsorption amount of PAAm-*g*-PEG can be seen in the pin-on-disk experiments. These results reveal that although PAAm-*g*-PEG of any grafting ratio lubricates much better than HEPES buffer solution alone, it still does not lubricate as well as PLL(20)-*g*[3.5]-PEG, which is consistent with the fact that PAAm-*g*-PEG does not adsorb as well or form as dense a PEG film as PLL-*g*-PEG. Yet the rolling friction results in Fig. 3 indicate that PAAm-*g*-PEG can lubricate as well as PLL(20)-*g*[3.5]-PEG.

An intrinsic difference between PAAm-*g*-PEG and PLL-*g*-PEG lies in the length of the spacer between the amine groups and the main backbone chain. While in the case of PLL-*g*-PEG the spacer consists of four methylene groups, only a single methylene separates the amine from the backbone in PAAm-*g*-PEG. The consequence of this difference is the greater flexibility of PLL-*g*-PEG in attaching to the negatively charged surface via its charged amines. Greater flexibility of the amine groups leads to a larger total number of attached anchoring sites per backbone at any given time, which in turn influences the total adsorption energy and thus the driving force for adsorption. This can, in turn, influence the advantageous "self-healing" effect [10] seen in PLL-*g*-PEG due to the polycationic backbone. In the presence of significant shear forces, the individual electrostatic interactions can be sequentially broken, leading to detachment, generally followed by subsequent readsorption of another polymer molecule.

In the case of sliding friction, during which the polymer layers are subject to continuous removal through tribological contact, both the surface binding energy of the polymer as well as its readsorption kinetics from solution ("self-healing" [10]) are critical in maintaining lubrication. The kinetics of readsorption, in turn, depends significantly on the ability of the polymers' anchoring groups to access surface countercharges. In the case of rolling friction, however, the shear forces are lower and therefore copolymer removal and subsequent self-healing processes are of secondary importance. In this case, the behavior of PLL-*g*-PEG and PAAm-*g*-PEG are similar.

The differences in adsorption and lubrication behavior of PAAm-*g*-PEG and PLL-*g*-PEG suggest that the chemical structure of the backbone plays an important role in lubrication and adsorption in several ways. The shorter repeat-length of the PAAm backbone means that PAAm-*g*-PEG polymers have a greater number of binding groups (charges) per unit backbone length than a PLL-*g*-PEG with similar PEG spacing. Despite this, it appears that PAAm-*g*-PEG is adsorbed to a lesser extent and lubricates less well in sliding geometry than the equivalent PLL-*g*-PEG (with similar PEG spacing along the backbone). We therefore hypothesize that the longer spacers to the amine groups on PLL allow these anchoring sites more degrees of freedom to attach to the surface, increasing the total bond strength and accelerating adsorption kinetics, especially on real surfaces, which may contain inhomogeneities and may not be atomically flat. The flexible spacer on the PLL backbone may also promote better packing of the films, increasing the PEG coverage on the surface and therefore a more effective tribofilm.

5 Conclusion

The chemical structure of the anchoring group of polycationic polymer brushes significantly influences their performance as aqueous lubricant additives. The longer spacer in the anchoring group of PLL-*g*-PEG improves its lubrication performance in three major ways. First, the flexible anchoring groups leads to a higher PEG chain density, leading to a greater brush thickness and concomitantly greater protection against asperity–asperity contact. Second, the overall surface binding energy of the polymer is increased by the longer spacer in the anchoring group, which leads to a greater number of surface attachments and thus reduces tribo-induced desorption. Finally, the increased binding energy also increases the rate of polymer readsorption, increasing the self-healing effect of the PLL-*g*-PEG.

Acknowledgment The authors would like to thank the Research Commission of the ETH Zurich for funding.

References

1. Klein, J., Luckham, P.F.: Forces between two adsorbed poly(ethylene oxide) layers in a good aqueous solvent in the range 0–150 nm. Macromolecules **17**, 1041–1048 (1984). doi:10.1021/ma00135a011
2. Taunton, H.J., Toprakcioglu, C., Fetters, L.J., Klein, J.: Interactions between surfaces bearing end-adsorbed chains in a good solvent. Macromolecules **23**, 571–580 (1990). doi:10.1021/ma00204a033
3. Raviv, U., Frey, J., Sak, R., Laurat, P., Tadmor, R., Klein, J.: Properties and interactions of physigrafted end-functionalized poly(ethylene glycol) layers. Langmuir **18**, 7482–7495 (2002). doi:10.1021/la020002s
4. Lee, S., Muller, M., Ratoi-Salagean, M., Voros, J., Pasche, S., De Paul, S.M., et al.: Boundary lubrication of oxide surfaces by poly(L-lysine)-g-poly(ethylene glycol) (PLL-g-peg) in aqueous media. Tribol. Lett. **15**, 231–239 (2003). doi:10.1023/A:1024861119372
5. Muller, M., Lee, S., Spikes, H.A., Spencer, N.D.: The influence of molecular architecture on the macroscopic lubrication properties of the brush-like co-polyelectrolyte poly(L-lysine)-g-poly(ethylene glycol) (PLL-g-PEG) adsorbed on oxide surfaces. Tribol. Lett. **15**, 395–405 (2003). doi:10.1023/B:TRIL.0000003063.98583.bb
6. Lee, S., Iten, R., Muller, M., Spencer, N.D.: Influence of molecular architecture on the adsorption of poly(ethylene oxide)-poly(propylene oxide)-poly(ethylene oxide) on pdms surfaces and implications for aqueous lubrication. Macromolecules **37**, 8349–8356 (2004). doi:10.1021/ma049076w
7. Yan, X., Perry, S.S., Spencer, N.D., Pasche, S., DePaul, S.M., Textor, M., et al.: Reduction of friction at oxide interfaces upon polymer adsorption from aqueous solutions. Langmuir **20**, 423–428 (2004). doi:10.1021/la035785b
8. Muller, M.T., Yan, X., Lee, S., Perry, S.S., Spencer, N.D.: Preferential solvation and its effect on the lubrication properties of a surface-bound, brushlike copolymer. Macromolecules **38**, 3861–3866 (2005). doi:10.1021/ma047468x
9. Muller, M.T., Yan, X., Lee, S., Perry, S.S., Spencer, N.D.: Lubrication properties of a brushlike copolymer as a function of the amount of solvent absorbed within the brush. Macromolecules **38**, 5706–5713 (2005). doi:10.1021/ma0501545
10. Lee, S., Muller, M., Heeb, R., Zurcher, S., Tosatti, S., Heinrich, M., et al.: Self-healing behavior of a polyelectrolyte-based lubricant additive for aqueous lubrication of oxide materials. Tribol. Lett. **24**, 217–223 (2006). doi:10.1007/s11249-006-9121-9
11. Lee, S., Spencer, N.D.: Aqueous lubrication of polymers: influence of surface modification. Tribol. Int. **38**, 922–930 (2006). doi:10.1016/j.triboint.2005.07.017
12. Drobek, T., Spencer, N. D.: Nanotribology of surface-grafted peg layers in an aqueous environment. Langmuir **24**, 1484–1488 (2008)
13. Lee, S., Spencer, N.D.: Poly(L-lysine)-graft-poly(ethylene glycol): a versatile aqueous lubricant additive for tribosystems involving thermoplastics. Lubrication Sci. **20**, 21–34 (2008)
14. Lee, S., Spencer, N.D.: Achieving ultralow friction by aqueous, brush-assisted lubrication. In: Erdemir A., Martin J.-M., (eds) Superlubricity. Elsevier Science (2007)
15. Lee, S., Spencer, N.D.: Materials science: sweet, hairy, soft, and slippery. Science **319**, 575–576 (2008). doi:10.1126/science.1153273
16. Elbert, D.L., Hubbell, J.A.: Self-assembly and steric stabilization at heterogeneous, biological surfaces using adsorbing block copolymers. Chem. Biol. **5**, 177–183 (1998). doi:10.1016/S1074-5521(98)90062-X
17. Kenausis, G.L., Voros, J., Elbert, D.L., Huang, N., Hofer, R., Ruiz-Taylor, L., et al.: Poly(L-lysine)-g-Poly(ethylene glycol) layers on metal oxide surfaces: attachment mechanism and effects of polymer architecture on resistance to protein adsorption. J. Phys. Chem B **104**, 3298–3309 (2000). doi:10.1021/jp993359m
18. Heuberger, M.: The extended surface forces apparatus. Part I. Fast spectral correlation interferometry. Rev. Sci. Instrum. **72**, 1700–1707 (2001). doi:10.1063/1.1347978
19. Huang, N.P., Michel, R., Voros, J., Textor, M., Hofer, R., Rossi, A., et al.: Poly(L-lysine)-g-poly(ethylene glycol) layers on metal oxide surfaces: surface-analytical characterization and resistance to serum and fibrinogen adsorption. Langmuir **17**, 489–498 (2001). doi:10.1021/la000736±
20. Huang, N.P., Csucs, G., Emoto, K., Nagasaki, Y., Kataoka, K., Textor, M., et al.: Covalent attachment of novel poly(ethylene glycol)-poly(DL-lactic acid) copolymeric micelles to TiO2 surfaces. Langmuir **18**, 252–258 (2002). doi:10.1021/la0109563
21. Huang, N.P., Voros, J., De Paul, S.M., Textor, M., Spencer, N.D.: Biotin-derivatized poly(L-lysine)-g-poly(ethylene glycol): a novel polymeric interface for bioaffinity sensing. Langmuir **18**, 220–230 (2002). doi:10.1021/la010913m
22. Michel, R., Reviakine, I., Sutherland, D., Fokas, C., Csucs, G., Danuser, G., et al.: A novel approach to produce biologically relevant chemical patterns at the nanometer scale: selective molecular assembly patterning combined with colloidal lithography. Langmuir **18**, 8580–8586 (2002). doi:10.1021/la0258244
23. Muller, M., Voros, J., Csucs, G., Walter, E., Danuser, G., Merkle, H.P., et al.: Surface modification of PLGA microspheres. J. Biomed. Mater. Res A **66A**, 55–61 (2003). doi:10.1002/jbm.a.10502
24. Pasche, S., De Paul, S.M., Voros, J., Spencer, N.D., Textor, M.: Poly(L-lysine)-graft-poly(ethylene glycol) assembled monolayers on niobium oxide surfaces: a quantitative study of the influence of polymer interfacial architecture on resistance to protein adsorption by ToF-SIMS and in situ OWLS. Langmuir **19**, 9216–9225 (2003). doi:10.1021/la034111y
25. Tosatti, S., De Paul, S.M., Askendal, A., VandeVondele, S., Hubbell, J.A., Tengvall, P.: Peptide functionalized poly(L-lysine)-g-poly(ethylene glycol) on titanium: resistance to protein adsorption in full heparinized human blood plasma. Biomaterials **24**, 4949–4958 (2003). doi:10.1016/S0142-9612(03)00420-4
26. VandeVondele, S., Voros, J., Hubbell, J.A.: RGD-Grafted poly-L-lysine-graft-(polyethylene glycol) copolymers block non-specific protein adsorption while promoting cell adhesion. Biotechnol. Bioeng. **82**, 784–790 (2003). doi:10.1002/bit.10625
27. Heuberger, M., Drobek, T., Voros, J.: About the role of water in surface-grafted poly(ethylene glycol) layers. Langmuir **20**, 9445–9448 (2004). doi:10.1021/la048384k
28. Wagner, M.S., Pasche, S., Castner, D.G., Textor, M.: Characterization of poly(L-lysine)-graft-poly(ethylene glycol) assembled monolayers on niobium pentoxide substrates using time-of-flight secondary ion mass spectrometry and multivariate analysis. Anal. Chem. **76**, 1483–1492 (2004). doi:10.1021/ac034873y
29. De Paul, S.M., Falconnet, D., Pasche, S., Textor, M., Abel, A.P., Kauffmann, E., et al.: Tuned graft copolymers as controlled coatings for DNA microarrays. Anal. Chem. **77**, 5831–5838 (2005). doi:10.1021/ac0504666
30. Drobek, T., Spencer, N.D., Heuberger, M., Compressing, P.E.G.: Brushes. Macromolecules **38**, 5254–5259 (2005). doi:10.1021/ma0504217

31. Feuz, L., Leermakers, F.A.M., Textor, M., Borisov, O.: Bending rigidity and induced persistence length of molecular bottle brushes: a self-consistent-field theory. Macromolecules **38**, 8891–8901 (2005). doi:10.1021/ma050871z
32. Heuberger, M., Drobek, T., Spencer, N.D.: Interaction forces and morphology of a protein-resistant poly(ethylene glycol) layer. Biophys. J. **88**, 495–504 (2005). doi:10.1529/biophysj.104.045443
33. Lee, S., Voros, J.: An aqueous-based surface modification of poly(dimethylsiloxane) with poly(ethylene glycol) to prevent biofouling. Langmuir **21**, 11957–11962 (2005). doi:10.1021/la051932p
34. Pasche, S., Textor, M., Meagher, L., Spencer, N.D., Griesser, H.J.: Relationship between interfacial forces measured by colloid-probe atomic force microscopy and protein resistance of poly(ethylene glycol)-grafted poly(L-lysine) adlayers on niobia surfaces. Langmuir **21**, 6508–6520 (2005). doi:10.1021/la050386x
35. Blattler, T.M., Pasche, S., Textor, M., Griesser, H.J.: High salt stability and protein resistance of poly(L-lysine)-g-poly(ethylene glycol) copolymers covalently immobilized via aldehyde plasma polymer interlayers on inorganic and polymeric substrates. Langmuir **22**, 5760–5769 (2006). doi:10.1021/la0602766
36. Morgenthaler, S., Zink, C., Stadler, B., Voros, J., Lee, S., Spencer, N.D., et al.: Poly(L-lysine)-grafted-poly(ethylene glycol)-based surface-chemical gradients. Preparation, characterization, and first applications. Biointerphases **1**, 156–165 (2006). doi:10.1116/1.2431704
37. Wattendorf, U., Koch, M.C., Walter, E., Voros, J., Textor, M., Merkle, H.P.: Phagocytosis of poly(L-lysine)-graft-poly(ethylene glycol) coated microspheres by antigen presenting cells: impact of grafting ratio and poly(ethylene glycol) chain length on cellular recognition. Biointerphases **1**, 123–133 (2006). doi:10.1116/1.2409645
38. Feuz, L., Strunz, P., Geue, T., Textor, M., Borisov, O.: Conformation of poly(L-lysine)-graft-poly(ethylene glycol) molecular brushes in aqueous solution studied by small-angle neutron scattering. Eur. Phys. J. E. Soft Matter **23**, 237–245 (2007)
39. Tleugabulova, D., Czardybon, W., Brennan, J.D.: Time-resolved fluorescence anisotropy in assessing side-chain and segmental motions in polyamines entrapped in sol-gel derived silica. J. Phys. Chem. B **108**, 10692–10699 (2004). doi:10.1021/jp0491109
40. Sawhney, A.S., Hubbell, J.A.: Poly(ethylene oxide)-graft-poly(L-lysine) copolymers to enhance the biocompatibility of poly(L-lysine)-alginate microcapsule membranes. Biomaterials **13**, 863–870 (1992). doi:10.1016/0142-9612(92)90180-V
41. Voros, J., Ramsden, J.J., Csucs, G., Szendro, I., De Paul, S.M., Textor, M., et al.: Optical grating coupler biosensors. Biomaterials **23**, 3699–3710 (2002). doi:10.1016/S0142-9612(02)00103-5
42. Kawaguchi, S., Imai, G., Suzuki, J., Miyahara, A., Kitano, T., Ito, K.: Aqueous solution properties of oligo- and poly(ethylene oxide) by static light scattering and intrinsic viscosity. Polymer (Guildf) **38**, 2885–2891 (1997). doi:10.1016/S0032-3861(96)00859-2
43. Alexander, S.: Adsorption of chain molecules with a polar head a-scaling description. J. Phys. **38**, 983–987 (1977)
44. de Gennes, P.G.: Polymers at an interface; a simplified view. Adv. Colloid Interface Sci. **27**, 189–209 (1987). doi:10.1016/0001-8686(87)85003-0
45. Szleifer, I., Carignano, M.A.: Tethered polymer layers: phase transitions and reduction of protein adsorption. Macromol. Rapid Commun. **21**, 423–448 (2000). doi:10.1002/(SICI)1521-3927(20000501)21:8<423::AID-MARC423>3.0.CO;2-J